

MIT Open Access Articles

Quenched-vacancy induced spin-glass order

The MIT Faculty has made this article openly available. **Please share** how this access benefits you. Your story matters.

Citation: Gulpinar, Gul, and A. Nihat Berker. "Quenched-vacancy induced spin-glass order." Physical Review E 79.2 (2009): 021110. © 2009 The American Physical Society.

As Published: <http://dx.doi.org/10.1103/PhysRevE.79.021110>

Publisher: American Physical Society

Persistent URL: <http://hdl.handle.net/1721.1/51803>

Version: Final published version: final published article, as it appeared in a journal, conference proceedings, or other formally published context

Terms of Use: Article is made available in accordance with the publisher's policy and may be subject to US copyright law. Please refer to the publisher's site for terms of use.



Quenched-vacancy induced spin-glass order

Gül Gülpınar^{1,2} and A. Nihat Berker^{3,2,4}

¹*Department of Physics, Dokuz Eylül University, Buca 35160, Izmir, Turkey*

²*Feza Gürsey Research Institute, TÜBİTAK—Bosphorus University, Çengelköy 34680, Istanbul, Turkey*

³*Department of Physics, Koç University, Sarıyer 34450, Istanbul, Turkey*

⁴*Department of Physics, Massachusetts Institute of Technology, Cambridge, Massachusetts 02139, USA*

(Received 31 October 2008; revised manuscript received 1 January 2009; published 9 February 2009)

The ferromagnetic phase of an Ising model in $d=3$, with any amount of quenched antiferromagnetic bond randomness, is shown to undergo a transition to a spin-glass phase under sufficient quenched bond dilution. This result, demonstrated here with the numerically exact global renormalization-group solution of a $d=3$ hierarchical lattice, is expected to hold true generally, for the cubic lattice and for quenched site dilution. Conversely, in the ferromagnetic–spin-glass–antiferromagnetic phase diagram, the spin-glass phase expands under quenched dilution at the expense of the ferromagnetic and antiferromagnetic phases. In the ferromagnetic–spin-glass phase transition induced by quenched dilution, reentrance as a function of temperature is seen, as previously found in the ferromagnetic–spin-glass transition induced by increasing the antiferromagnetic bond concentration.

DOI: 10.1103/PhysRevE.79.021110

PACS number(s): 64.60.ah, 75.10.Nr, 05.10.Cc, 75.50.Lk

The spin-glass phase [1] is much studied due to its prominent role in complex systems, as an example of random order. In its simplest realization in the Ising model, the underlying system has randomly distributed ferromagnetic and antiferromagnetic bonds. In spatial dimension $d=3$, at low temperatures, ferromagnetic or antiferromagnetic ordered phases occur when the system has predominantly (e.g., more than 77% [2]) ferromagnetic or antiferromagnetic bonds, respectively. In between, the spin-glass phase occurs. The occurrence of the spin-glass phase, in which the local degrees of freedom are frozen in random directions, has strong implications in physical systems that are realizations of the spin-glass system, spanning from materials science to information theory and neural networks.

We have studied possibly the simplest modification of the spin-glass system, to be commonly expected or realized in physical systems, namely, the removal of bonds. We find important qualitative and quantitative effects. This Ising spin-glass system with quenched bond vacancies [3–10] has the Hamiltonian

$$-\beta H = \sum_{\langle ij \rangle} K_{ij} s_i s_j, \quad (1)$$

where $s_i = \pm 1$ at each site i and $\langle ij \rangle$ indicates summation over nearest-neighbor pairs of sites. The local bond strengths are $K_{ij} = K > 0$ with probability p_+ , $K_{ij} = -K$ with probability p_- , or $K_{ij} = 0$ with probability $q = 1 - p_+ - p_-$, respectively corresponding to a ferromagnetic interaction, an antiferromagnetic interaction, or a bond vacancy. This model has previously been studied at zero temperature [6,9] and in its spin-glass phase diagram cross section [10] by position-space renormalization-group theory, in its n -replica version at zero temperature [3,5], by mean-field theory [4], and by momentum-space renormalization-group theory around $d=6$ dimensions [4], and by series expansion [7,8].

We have performed the numerically exact renormalization-group solution of this system on a $d=3$ hierarchical lattice [11–13], to be given below. Exact solutions

on hierarchical lattices constitute very good approximate solutions for physical lattices [14]. We calculate the global phase diagram in the variables of temperature $1/K$, bond vacancy concentration q , and antiferromagnetic bond fraction $p_-/(p_+ + p_-)$, obtaining a rich structure and finding reentrance as a function of temperature induced by bond vacancy. Our results agree with and extend the previous results [3–10] on this system.

Our results are most strikingly seen in Fig. 1. The top curve in Fig. 1(a) corresponds to the quenched dilution of the system with no antiferromagnetic bonds ($p_- = 0$). As the system is quenched diluted, by increasing the missing-bond concentration q , the transition temperature to the ferromagnetic phase is lowered from its value with no missing bonds at $q = 0$, until it reaches zero temperature and the ferromagnetic phase disappears at the percolation threshold of $q = 0.789$ (to be compared with the value of 0.753 in the simple cubic lattice [15]). However, with the inclusion of even the smallest amount of antiferromagnetic bonds (lower curves), a spin-glass phase, extending to finite temperatures, always appears before percolation. This result was previously obtained at zero temperature [3,6,7,9] and around $d=6$ [4].

The phase boundary between this vacancy-induced ferromagnetic–spin-glass phase transition shows reentrance, as also seen [16–18] in conventional spin-glass phase diagrams where the antiferromagnetic bond concentration is scanned. In Fig. 1(b), where the curves correspond to higher percentages of antiferromagnetic interactions among the bonds present, starting with $p_-/(p_+ + p_-) = 0.25$ in the top curve, the ferromagnetic phase has disappeared and only spin-glass ordering occurs. As seen from Fig. 1(a), the percolation threshold of the spin-glass phase is slightly lower than that of the pure ferromagnetic phase and, before the disappearance of the ferromagnetic phase, the percolation threshold of the spin-glass phase has a slight dependence on $p_-/(p_+ + p_-)$. The percolation threshold of the spin-glass phase settles to the value of 0.763 after the disappearance of the ferromagnetic phase.

Figure 2 shows the conventional phase diagrams of tem-

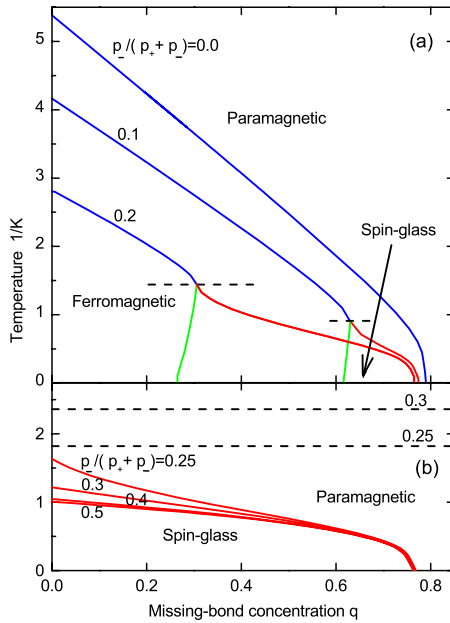


FIG. 1. (Color online) Calculated phase diagrams at constant $p_-(p_+ + p_-)$. All phase transitions (full lines) are second order. The dashed horizontal lines [shown only partly in (a)] are not phase boundaries, but the Nishimori symmetry lines, given by Eq. (2), for each value of $p_-(p_+ + p_-)$. The multicritical points in (a), mediating the ferromagnetic, spin-glass, and paramagnetic phases, occur on the Nishimori symmetry lines. These lines do not cross the phase boundaries at any other type of point. Thus, the Nishimori symmetry lines in (b) are at temperatures above the phase boundaries.

perature versus the fraction $p_-(p_+ + p_-)$ of antiferromagnetic bonds in the nonmissing bonds, at fixed values of the dilution q . As the dilution is increased, the phases are depressed in temperature, as can be expected. However, simultaneously, it is seen that the spin-glass phase expands [10] along the $p_-(p_+ + p_-)$ axis, at the expense of the ferromagnetic and antiferromagnetic phases, eventually dominating the entire low-temperature region. It is also seen, for $q=0.763$ and higher, that the spin-glass phase occurs in the phase diagrams as two disconnected regions, near the ferromagnetic and antiferromagnetic phases. A similar disconnected topology has recently been seen in the Blume-Emery-Griffiths spin glass [19].

The dashed lines in Figs. 1 and 2 are the Nishimori symmetry lines [20,21]

$$e^{\pm 2K} = \frac{p_+}{p_-}. \quad (2)$$

All multicritical points occurring in the currently studied system are on the Nishimori symmetry lines [22,23], as also previously seen [10] for this system. Thus, as illustrated in Fig. 2, it is possible to continuously populate, with multicritical points, the low-temperature segment of the Nishimori line, by gradually changing the quenched dilution q . The Nishimori symmetry condition appears in Fig. 1 as a horizontal line for each value of $p_-(p_+ + p_-)$. This horizontal line intersects the upper curve in Fig. 1(a) at zero temperature, thereby implying the occurrence of a zero-temperature mul-

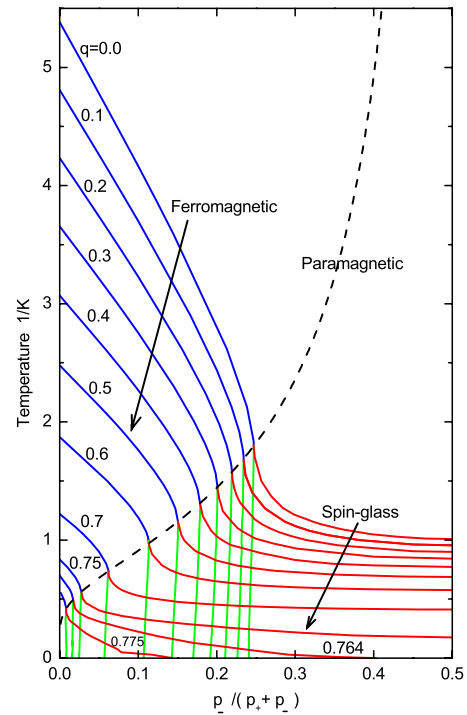


FIG. 2. (Color online) Calculated phase diagrams at constant quenched dilution $q = 1 - p_+ - p_-$. Since phase diagrams are symmetric about $p_-(p_+ + p_-) = 0.5$, with the antiferromagnetic phase replacing the ferromagnetic phase, only the $p_-(p_+ + p_-) < 0.5$ halves are shown. All phase transitions (full lines) are second order. The dashed curve is the Nishimori symmetry line given by Eq. (2). All multicritical points, mediating the ferromagnetic, spin-glass, and paramagnetic phases, lie on the Nishimori symmetry line.

ticritical point at the percolation threshold, as also deduced from the sequence of phase diagrams in Fig. 2. The horizontal lines of the Nishimori condition intersect the two other phase diagrams in Fig. 1(a) at their multicritical point. In Fig. 1(b), multicritical points do not occur and the horizontal lines of the Nishimori condition do not intersect the phase boundaries, occurring at higher temperatures than the phase boundaries.

Figure 3 shows the zero-temperature limit of the global phase diagram of the currently studied system. In the zero-temperature phase diagram, it is again seen that a spin-glass phase intervenes [3,6,7,9], with the smallest amount of quenched antiferromagnetic bonds, between the ferromagnetic phase and percolation, causing a direct ferromagnetic–spin-glass phase transition.

Our method, detailed in other works [19,24–26], will be briefly described now. We use the $d=3$ hierarchical lattice whose construction is given in Fig. 4. This hierarchical lattice has the odd rescaling factor of $b=3$, for the *a priori* equivalent treatment of ferromagnetism and antiferromagnetism, necessary for spin-glass problems. Hierarchical lattices admit exact solutions, by a renormalization-group transformation that reverses the construction steps [11–13]. Thus, hierarchical lattices have become the testing grounds for a large variety of cooperative phenomena, as also seen in recent works [14,27–37]. The hierarchical lattice of Fig. 4 has been used in this work, because it gives numerically accurate

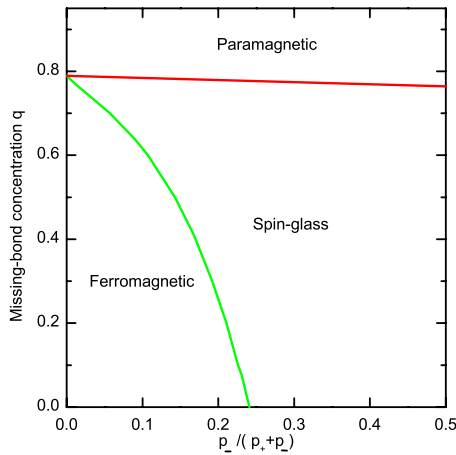


FIG. 3. (Color online) Calculated zero-temperature, $1/K=0$, phase diagram. All phase transitions are second order.

results for the critical temperatures of the $d=3$ isotropic and anisotropic Ising models on the cubic lattice [14].

In systems with quenched randomness, the renormalization-group transformation determines the mapping of the quenched probability distribution $\mathcal{P}(K)$ [38]. At each step, the innermost unit of the lattice as pictured on the right side of Fig. 4 is replaced by a single bond. This is effected by a series of pairwise convolutions of the quenched probability distributions,

$$\tilde{\mathcal{P}}(\tilde{K}) = \int dK^I dK^{II} \mathcal{P}_I(K^I) \mathcal{P}_{II}(K^{II}) \delta(\tilde{K} - R(K^I, K^{II})), \quad (3)$$

where $R(K^I, K^{II})$ is

$$R(K_{ij}^I, K_{ij}^{II}) = K_{ij}^I + K_{ij}^{II} \quad (4)$$

for replacing two in-parallel random bonds with distributions $\mathcal{P}_I(K^I)$ and $\mathcal{P}_{II}(K^{II})$ by a single bond with $\tilde{\mathcal{P}}(\tilde{K})$, or

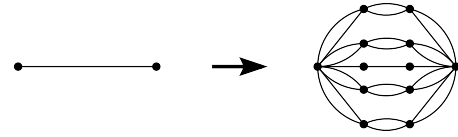


FIG. 4. The $d=3$ hierarchical lattice for which our calculation is exact is constructed by the repeated embedding of the graph as shown in this figure. This hierarchical lattice gives numerically accurate results for the critical temperatures of the $d=3$ isotropic and anisotropic Ising models on the cubic lattice [14].

$$R(K_{ij}^I, K_{jk}^{II}) = \frac{1}{2} \ln \left(\frac{\cosh(K_{ij}^I + K_{jk}^{II})}{\cosh(K_{ij}^I - K_{jk}^{II})} \right) \quad (5)$$

for replacing two in-series random bonds by a single bond. The probability distributions are in the form of probabilities assigned to interaction values, namely, histograms. Starting with the three histograms described after Eq. (1), the number of histograms quickly increases under the convolutions described above. At the computational limit, a binning procedure is used before each convolution to combine nearby histograms [19,24–26], so that 160 000 histograms are kept to describe the probability distributions. The flows of these probability distributions, under iterated renormalization-group transformations, determine the global phase diagram of the system.

This research was supported by the Scientific and Technological Research Council of Turkey (TÜBİTAK), including computational support through the TR-Grid e-Infrastructure Project hosted by ULAKBİM, and by the Academy of Sciences of Turkey. G.G. gratefully acknowledges support by the TÜBİTAK-BİDEP.

-
- [1] H. Nishimori, *Statistical Physics of Spin Glasses and Information Processing* (Oxford University Press, Oxford, 2001).
- [2] Y. Ozeki and N. Ito, *J. Phys. A* **31**, 5451 (1998).
- [3] A. Aharony, *J. Phys. C* **11**, L457 (1978).
- [4] M. R. Giri and M. J. Stephen, *J. Phys. C* **11**, L541 (1978).
- [5] A. Aharony and P. Pfeuty, *J. Phys. C* **12**, L125 (1979).
- [6] B. W. Southern, A. P. Young, and P. Pfeuty, *J. Phys. C* **12**, 683 (1979).
- [7] A. Aharony and K. Binder, *J. Phys. C* **13**, 4091 (1980).
- [8] R. G. Palmer and F. T. Bantilan, Jr., *J. Phys. C* **18**, 171 (1985).
- [9] A. J. Bray and S. Feng, *Phys. Rev. B* **36**, 8456 (1987).
- [10] E. J. Hartford and S. R. McKay, *J. Appl. Phys.* **70**, 6068 (1991).
- [11] A. N. Berker and S. Ostlund, *J. Phys. C* **12**, 4961 (1979).
- [12] R. B. Griffiths and M. Kaufman, *Phys. Rev. B* **26**, 5022 (1982).
- [13] M. Kaufman and R. B. Griffiths, *Phys. Rev. B* **30**, 244 (1984).
- [14] A. Erbaş, A. Tuncer, B. Yücesoy, and A. N. Berker, *Phys. Rev. E* **72**, 026129 (2005).
- [15] J. W. Essam, in *Phase Transitions and Critical Phenomena*, edited by C. Domb and M. S. Green (Academic, London, 1972), Vol. 2, pp. 197–270.
- [16] G. Migliorini and A. N. Berker, *Phys. Rev. B* **57**, 426 (1998).
- [17] F. D. Nobre, *Phys. Rev. E* **64**, 046108 (2001).
- [18] S. B. Roy and M. K. Chattopadhyay, arXiv:0810.5215v1.
- [19] V. O. Özçelik and A. N. Berker, *Phys. Rev. E* **78**, 031104 (2008).
- [20] H. Nishimori, *J. Phys. C* **13**, 4071 (1980).
- [21] H. Nishimori, *Prog. Theor. Phys.* **66**, 1169 (1981).
- [22] P. Le Doussal and A. Georges, Yale University Report No. YCTPP1-88, 1988 (unpublished).
- [23] P. Le Doussal and A. B. Harris, *Phys. Rev. Lett.* **61**, 625 (1988).
- [24] A. Falicov and A. N. Berker, *Phys. Rev. Lett.* **76**, 4380 (1996).
- [25] M. Hinczewski and A. N. Berker, *Phys. Rev. B* **72**, 144402 (2005).
- [26] C. Güven, A. N. Berker, M. Hinczewski, and H. Nishimori, *Phys. Rev. E* **77**, 061110 (2008).

- [27] M. Hinczewski and A. N. Berker, Phys. Rev. E **73**, 066126 (2006).
- [28] M. Hinczewski, Phys. Rev. E **75**, 061104 (2007).
- [29] Z. Z. Zhang, Z. G. Zhou, and L. C. Chen, Eur. Phys. J. B **58**, 337 (2007).
- [30] E. Khajeh, S. N. Dorogovtsev, and J. F. F. Mendes, Phys. Rev. E **75**, 041112 (2007).
- [31] H. D. Rozenfeld and D. ben-Avraham, Phys. Rev. E **75**, 061102 (2007).
- [32] M. Kaufman and H. T. Diep, J. Phys.: Condens. Matter **20**, 075222 (2008).
- [33] F. A. P. Piolho, F. A. da Costa, and C. G. Bezerra, Physica A **387**, 1538 (2008).
- [34] N. S. Branco, J. R. de Sousa, and A. Ghosh, Phys. Rev. E **77**, 031129 (2008).
- [35] T. Jorg and F. Ricci-Tersenghi, Phys. Rev. Lett. **100**, 177203 (2008).
- [36] S. Boettcher, B. Goncalves, and J. Azaret, J. Phys. A: Math. Theor. **41**, 335003 (2008).
- [37] C. Monthus and T. Garel, J. Phys. A: Math. Theor. **41**, 375005 (2008).
- [38] D. Andelman and A. N. Berker, Phys. Rev. B **29**, 2630 (1984).